

Factors secreted from dental pulp stem cells show multifaceted benefits for treating experimental temporomandibular joint osteoarthritis

N. Ogasawara †‡, F. Kano †, N. Hashimoto †, H. Mori §, Y. Liu †‡, L. Xia †‡, T. Sakamaki ‡, H. Hibi ||, T. Iwamoto §, E. Tanaka ‡, A. Yamamoto †*

† Department of Tissue Regeneration, Institute of Biomedical Sciences, Tokushima University Graduate School, 3-18-15 Kuramoto-cho, Tokushima, 770-8504, Japan

‡ Department of Orthodontics and Dentofacial Orthopedics, Institute of Biomedical Sciences, Tokushima University Graduate School, 3-18-15 Kuramoto-cho, Tokushima, 770-8504, Japan

§ Department of Pediatric Dentistry, Institute of Biomedical Sciences, Tokushima University Graduate School, 3-18-15 Kuramoto-cho, Tokushima, 770-8504, Japan

|| Department of Oral and Maxillofacial Surgery, Nagoya University Graduate School of Medicine, 65 Tsurumai-cho, Showa-ku, Nagoya, 466-8550, Japan



ARTICLE INFO

Article history:

Received 3 September 2019

Accepted 19 March 2020

Keywords:

Dental pulp stem cell
Conditioned medium
Chondrocyte
Cartilage regeneration
Temporomandibular joint
Osteoarthritis

SUMMARY

Objective: Temporomandibular joint osteoarthritis (TMJOA) is a degenerative disease characterized by progressive cartilage degeneration, abnormal bone remodeling, and chronic pain. In this study, we aimed to investigate effective therapies to reverse or suppress TMJOA progression.

Design: To this end, we performed intravenous administration of serum free conditioned media from human exfoliated deciduous teeth stem cells (SHED-CM) into a mechanical-stress induced murine TMJOA model.

Results: SHED-CM administration markedly suppressed temporal muscle inflammation, and improved bone integrity and surface smoothness of the destroyed condylar cartilage. Moreover, SHED-CM treatment decreased the number of IL-1 β , iNOS, and MMP-13 expressing chondrocytes, whereas it specifically increased PCNA-positive cells in the multipotent polymorphic cell layer. Notably, the numbers of TdT-mediated dUTP nick end labeling (TUNEL)-positive apoptotic chondrocytes in the SHED-CM treated condyles were significantly lower than in those treated with DMEM, whereas the proteoglycan positive area was restored to a level similar to that of the sham treated group, demonstrating that SHED-CM treatment regenerated the mechanical-stress injured condylar cartilage and subchondral bone. Secretome analysis revealed that SHED-CM contained multiple therapeutic factors that act in osteochondral regeneration.

Conclusions: Our data demonstrated that SHED-CM treatment promoted the regeneration and repair of mechanical-stress induced mouse TMJOA. Our observations suggest that SHED-CM has potential to be a potent tissue-regenerating therapeutic agent for patients with severe TMJOA.

© 2020 Osteoarthritis Research Society International. Published by Elsevier Ltd. All rights reserved.

* Address correspondence and reprint requests to: A. Yamamoto, Department of Tissue Regeneration, Institute of Biomedical Sciences, Tokushima University Graduate School, 3-18-15 Kuramoto-cho, Tokushima, 770-8504, Japan.

E-mail addresses: c301651009@tokushima-u.ac.jp (N. Ogasawara), fkano@tokushima-u.ac.jp (F. Kano), nhashimoto@tokushima-u.ac.jp (N. Hashimoto), h.mori@tokushima-u.ac.jp (H. Mori), c301751019@tokushima-u.ac.jp (Y. Liu), c301951003@tokushima-u.ac.jp (L. Xia), sakuma.takuma@tokushima-u.ac.jp (T. Sakamaki), hibihi@med.nagoya-u.ac.jp (H. Hibi), iwamoto@tokushima-u.ac.jp (T. Iwamoto), etanaka@tokushima-u.ac.jp (E. Tanaka), akihito@tokushima-u.ac.jp (A. Yamamoto).

Introduction

The temporomandibular joint (TMJ) is a load-bearing articulation with a wide range of motion consisting of both rotation and translation. The articular cartilage in general synovial joints is a thin layer of hyaline cartilage that covers the entire articulating surface of each bone. The mandibular condylar cartilage however, uniquely consists of four layers: 1) a superficial fibrous layer covering the articular, 2) a proliferating polymorphic cell layer having multilineage differentiation potency toward osteoblasts, chondrocytes,

and adipocytes, 3) a mature hyaline-like cartilage layer producing cartilage matrix, and 4) a hypertrophic cell layer initiating endochondral ossification¹. This heterogeneous architecture plays an important role in maintaining condylar structure and function in the face of mechanical stress.

TMJ osteoarthritis (TMJOA) is a degenerative joint disease, characterized by progressive cartilage degeneration, abnormal bone remodeling, and chronic pain². The etiology of TMJOA is complex and multifactorial. However, it has been suggested that excessive malocclusion-induced mechanical stress affects TMJOA progression². It has also been shown that injury-activated chondrocytes play important roles in the pathophysiology of early stage TMJOA. Activated chondrocytes increase production of cartilage-degrading catabolic enzymes, proinflammatory cytokines, oxidative stress-inducers, and osteoclast-activators, such as matrix metalloproteinase-13 (MMP-13), interleukin-1 β (IL-1 β), inducible nitric oxide synthase (iNOS), and receptor activator of nuclear factor (NF)- κ B ligand (RANKL), respectively. During the progression phase, these tissue-degenerative TMJOA microenvironments promote degradation of cartilage matrix, chondrocyte apoptosis and necrosis, and abnormal resorption of subchondral bone, leading to irreversible articular damage and functional impairment^{3,4}. As the self-repair capability of the articular cartilage is limited, development of effective therapies to reverse or suppress TMJOA progression are currently under investigation.

Stem cell therapy holds great promise for the development and establishment of effective treatments for TMJOA and osteoarthritis (OA). It has been shown that transplantation of undifferentiated adult mesenchymal stem cells (MSCs) isolated from adipose tissue or bone marrow improved the OA-phenotype in clinical studies of animal TMJOA and Knee-OA models^{5,6}. However, most of these studies reported poor cell graft survival, suggesting that recovery of articular damage was primarily accomplished through paracrine trophic mechanisms. Stem cells secrete a broad repertoire of trophic and immunomodulatory factors, which can be collected as a serum-free conditioned medium (CM). Conditioned media from various stem cell types have been shown to exhibit considerable potential in treating a myriad of intractable diseases⁷.

Human adult dental pulp stem cells (DPSCs) and stem cells from human exfoliated deciduous teeth (SHED) are self-renewing MSCs residing within the perivascular niche of the dental pulp. These cells are thought to originate from the cranial neural crest, which expresses early markers for both MSCs and neuroectodermal stem cells⁸. Implantation of DPSCs, pre-differentiated toward chondrocytes, resulted in significant cartilage regeneration in a rabbit model of knee cartilage damage⁹. The study demonstrated the therapeutic potential of local delivery of *ex vivo* culture-expanded DPSCs for treating OA. However, the benefits of these DPSC-secreted factors in the treatment of TMJOA, have not been examined. Notably, systemic administration of SHED serum free conditioned medium (SHED-CM) promoted functional recovery in various acute and chronic intractable disease models¹⁰, such as ischemic brain injury¹¹, Alzheimer's disease¹², spinal cord injury¹³, fulminant liver failure¹⁴, liver fibrosis¹⁵, bleomycin-induced fibrotic lung injury¹⁶, autoimmune encephalomyelitis¹⁷, type I diabetes¹⁸, rheumatoid arthritis¹⁹, and cardiac injury²⁰. In the present study, we investigated the therapeutic effects of SHED-CM administration in a mouse mechanical stress-induced TMJOA experimental model.

Methods

Preparation of SHED-CM

Human SHEDs were isolated and cultured as previously described⁸. In brief, deciduous teeth from six- to twelve-year-old

individuals were collected at Nagoya University and Tokushima University Hospital. This study was approved by the Institutional Ethical Committee of Nagoya University and Tokushima University Hospital and performed according to the principles of the Declaration of Helsinki (Permit No H-73 and No: 3,268 for Nagoya and Tokushima University, respectively). The pulp was gently removed and digested for 1 h at 37 °C in a solution containing collagenase type I (3 mg/ml) and dispase (4 mg/ml). Single-cell suspensions were plated on culture dishes in Dulbecco's Modified Eagle Medium (DMEM) supplemented with 10 % fetal bovine serum (FBS), then incubated at 37 °C in 5 % CO₂. The human skin fibroblast line, derived from a 36-year-old individual, was obtained at passage 12 from the Health Science Research Resources Bank (Osaka, Japan). SHED (passage 9) and fibroblasts (passage 13) for CM preparation were seeded at 1×10^5 cells per dish. Cells at 70–80 % confluence were washed with phosphate-buffered saline (PBS) and serum-free DMEM twice, followed by culture media replacement with serum-free DMEM. Media were incubated for 48 h at 37 °C in a humidified atmosphere of 5 % CO₂, then collected and centrifuged for 3 min at 440 g and 4 °C^{8,13}. Supernatants were then used as SHED-CM in TMJOA treatment protocols. We adjusted the protein concentration of each CM to 3 μ g/ml with serum-free DMEM.

Mouse mechanical stress-induced TMJOA model and treatment with SHED-CM

Institute of Cancer Research (ICR) male mice, aged 11 weeks, were purchased from Japan SLC Inc (Shizuoka, Japan), kept individually in plastic cages, and maintained at ambient temperature (22–24 °C) in a 12 h light/dark cycle. Mice were fed a standard solid diet with water *ad libitum* throughout the experiment and were randomly divided into one control and three experimental groups ($n =$ five for each group). An overview of the experimental design and workflow is presented in [Supplemental Fig. 1](#).

In the experimental groups, mechanical stress was applied to both TMJs by forced mouth opening for 3 h/day for five or 10 consecutive days by using a custom-made spring. This device kept the mandible in a maximal mouth opening position of 14 mm, and delivered a force of 2 N on each TMJ [Fig. 1\(A\)](#)²¹. For the mouth opening experiments, mice were anaesthetized with a mixture of medetomidine (Domitor, Orion Corporation, Espoo, Finland), midazolam (Midazolam, Meiji Seika Pharma, Tokyo, Japan) and butorphanol (Vetorphale, Meiji Seika Pharma, Tokyo, Japan) at doses of 0.75, 4.0 and 5.0 mg/kg, respectively.

In one experimental group, both TMJs received only mechanical stress for 5 days only (pre-treatment group), while those in the other experimental groups received mechanical stress for 10 consecutive days and were injected daily with either 0.5 ml SHED-CM (SHED-CM group) or 0.5 ml DMEM (DMEM group) into the tail vein, from day six to day 10 [Fig. 1 \(B\)](#). For immunohistological analysis (except Proliferating Cell Nuclear Antigen, PCNA), mechanical stress followed by SHED-CM or DMEM treatment was carried out for three consecutive days [Fig. 1 \(C\)](#). For PCNA evaluation, mechanical stress was carried out for 6 days and mice received SHED-CM or DMEM on the last day [Fig. 1 \(D\)](#). When the animals were sacrificed, blood plasma was isolated and sent to SRL, Inc (Tokyo, Japan) where the level of C-reactive protein (CRP) was determined. Although no mechanical stress was applied to the TMJs of mice in the control group, the same anesthesia schedule was maintained. The weight of each mouse was measured immediately before the experiment (day 0), at the initial day of injection (day 6), and at the end of the experiment (day 10). All procedures performed in this study were approved by the Tokushima University Animal Care and Use Committee (Permit No: T30-95) and carried

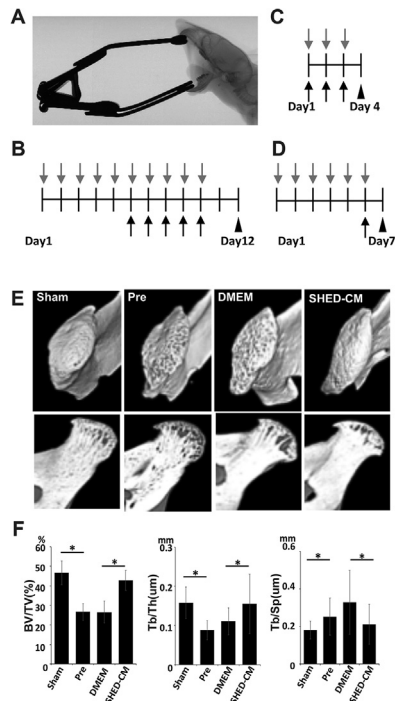


Fig. 1

SHED-CM restores TMJ subchondral bone volume and architecture in OA. (A) Mice were subjected to jaw-opening devices applied to the interincisal teeth to hold the mandible in the maximal opened position. (B–D) Experimental designs. Mechanical overloading was applied to both TMJs by forced mouth opening for 3 h/day. Gray and black arrows represent mechanical stress and treatment with DMEM or SHED-CM, respectively. CT, HE and TB staining, TUNEL and TRAP analysis were carried out by protocol. (E) Immunohistological analysis of MMP13, iNOS and IL-1 β , and of PCNA were carried out by (C) and (D), respectively. (F) Mice TMJs were harvested for micro-CT analysis at 12 days. Based on a 3D reconstruction section of mandibular condyles from TMJs, representative sagittal views from micro-CT scans of the condyles are shown. (F) Ratios of bone volume (BV/TV), trabecular thickness (Tb/Th) and trabecular separation (Tb/Sp). Data represent mean \pm s.e.m. ($n = 5/\text{group}$). ** $p < 0.01$.

Osteoarthritis
and Cartilage

out according to the Animal Research: Reporting of In Vivo Experiments (ARRIVE) guidelines.

Pain behavioral measurement

Mechanical hyper-nociception was assessed using the von Frey microfilament procedure under blind conditions²². A series of calibrated von Frey filaments (Aesthesio, Dammic global, CA, USA) were applied to the TMJ region. The head withdrawal threshold is defined as the lowest force applied by the filaments that produced a withdrawal response at least three times. Assessment of mechanical hyper-nociception were performed every day and the head withdrawal threshold was calculated as the mean value per joint of five mice per group.

Micro-computed tomography (Micro-CT) analysis

Murine mandibles from mice of all groups were resected, and the condyles were carefully separated from the soft surrounding tissues and fixed overnight in 70 % ethanol. Condyles were then analyzed using high-resolution micro-CT (SkyScan 1,176 scanner and associated analysis software; Buruker, Billerica, MA, USA). Image acquisition was performed at 50 kV and 200 μ A. During image acquisition, samples were tightly covered with plastic wrap to prevent movement and dehydration. To segment the bone image from background noise, thresholding was applied. The posterior region of the mandibular condyle in the midsagittal section was the region of interest (ROI). The resolution of the captured micro-CT images was 9 μ m/pixel. For each ROI, microstructural parameters including the bone volume to trabecular volume ratio (BV/TV), trabecular thickness (Tb.Th), and trabecular separation (Tb.Sp) were analyzed.

Histology and immunohistochemical analysis

Following micro-CT examination, fixed TMJ specimens were decalcified in 30 % ethylene diamine tetra acetic acid (EDTA) for 2 weeks prior to histology processing. Samples were dehydrated and embedded in paraffin for microtomy processing according to standard procedures. Tissue segments were isolated from three mice per experimental group, and subsequently, 5 μ m sagittal sections were generated. Sections were deparaffinized and hydrated through immersion in a series of xylene and graded alcohol solutions. Sections were stained with hematoxylin and eosin (HE) for histological assessment and with toluidine blue (TB) for visualizing proteoglycans. Tartrate-resistant acid phosphatase (TRAP) staining identifying active bone-absorbing osteoclasts was carried out using a TRAP/AP staining kit (Wako, Osaka, Japan) according to the manufacturer's instructions. Apoptotic cell death was analyzed using the TdT-mediated dUTP nick end labeling (TUNEL) assay (*In situ* Cell Death Detection Kit, Roche Life Science, Geneva, Switzerland) according to the manufacturer's instruction.

For immunohistochemical analysis, sections were blocked with 5 % (v/v) bovine serum albumin for 30 min, and incubated overnight with the following primary antibodies: rabbit anti-MMP13 IgG (1:100, ab75606, Abcam, Cambridge, UK), rabbit anti-iNOS IgG (1:500, ab3523, Abcam), rabbit anti-IL-1 β IgG (1 μ g/ml, ab9722, Abcam), and rabbit anti-PCNA IgG (1:250, ab92552, Abcam). As secondary antibody, the anti-rabbit IgG (VECTASTAIN Elite ABC, Vector Laboratories) was used and processed by diaminobenzidine (DAB) staining using the ABC reaction protocol (Vector Laboratories). After counterstaining with Mayer Haematoxylin (Sakura Finetek Japan Co, Tokyo, Japan), tissue images

were captured using a universal fluorescence microscope (BZ9000; Keyence, Osaka, Japan). Time schedules of immunohistochemical staining for MMP13, iNOS, IL-1 β and PCNA evaluation are presented in Fig. 1(B) and (C), respectively. Cells were counted in at least five images captured from three individual specimens in parallel experiments.

LC-MS/MS analysis

Secretome analysis of CM was performed according to a previously reported protocol²³. In brief, SHED-CM and fibroblast-CM (Fibro-CM) were concentrated using Amicon Ultra 3K filter (Millipore, Burlington, MA, US). For protein purification, methanol/chloroform precipitation was performed. Resulting pellets were

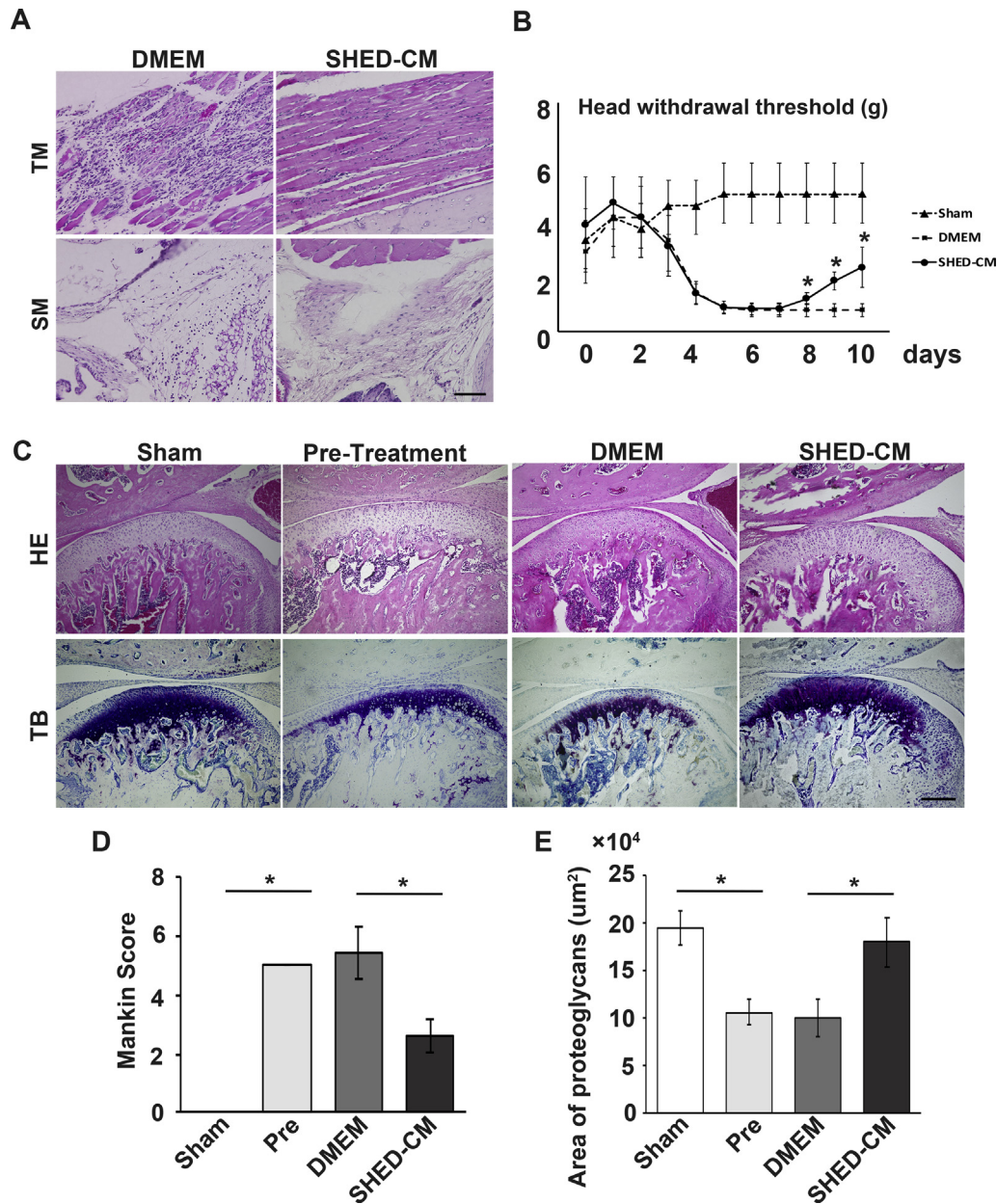


Fig. 2

Histopathological evaluation of TMJ repair by SHED-CM administration. (A) HE stained sections of temporal muscle (TM) and synovial membrane (SM). Scale bar: 50 μm . (B) Time-dependent nociceptive responses after treatment with SHED-CM. Head withdraw threshold of Sham, DMEM and SHED-CM group were measured. Data represent mean \pm s.e.m. ($n = 5/\text{group}$). * $p < 0.05$ compared to DMEM group (C). HE and toluidine blue (TB) staining of TMJ. Note, that SHED-CM treatment restored the cartilage layer thickness and chondrocyte alignment regularities. Scale bar: 100 μm . (D) Depicted scores are modified Mankin morphological scores. (E) The area (μm^2) stained for TB in the mandibular condylar cartilage tissues obtained from four experimental groups of TMJOA mice is illustrated. Data represent the mean \pm s.e.m. ($n = 5/\text{group}$). ** $p < 0.01$.

resolved by MS buffer (8 M urea and 50 mM Tris–HCl pH 8.0), followed by reduction in 5 mM DTT (WAKO, Osaka, Japan) and alkylation in 27.5 mM iodoacetamide (WAKO, Osaka, Japan) for 30 min in the dark at room temperature. After being diluted 8 times in 50 mM Tris–HCl pH 8.0, proteins were digested with 50 ng Lys-C (WAKO, Osaka, Japan) and trypsin (Promega, Madison, WI, US) at 37 °C overnight. Peptides were purified by GL-Tips SDB (GL science, Tokyo, Japan) according to the manufacturer's protocol. The concentration of peptides was measured using the Pierce™ Quantitative Colorimetric Peptide Assay Kit (Thermo, Waltham, MA, USA). Subsequently, peptides (268 ng each) were injected to an EASY-nLC™ connected to a Q-Exactive PLUS™ (Thermo) mass spectrometry system. Protein identification and label-free quantification were performed by Proteome Discoverer 2.2™ (Thermo).

Statistical analysis

The SPSS software package, version 22.0 (IBM, New York, USA) was used for statistical analysis. All data are expressed as the mean \pm standard error of the mean (SEM). Differences between groups were compared using the Student's *t* test or Mann–Whitney *U* test, according to the data type. To analyze three or more independent groups, we used repeated-measures analysis of variance (ANOVA) with Tukey's post hoc test. A *p* value < 0.05 was considered to be statistically significant.

Results

SHED-CM restored bone integrity and surface properties of condyles in mice with TMJOA

Micro-CT images revealed a rougher condylar cartilage surface with severe subchondral trabecular bone loss in the pre-treatment and DMEM groups, whereas that of the SHED-CM group had a smoother surface and decreased subchondral trabecular bone resorption [Fig. 1 (E)]. We also measured BV/TV, Tb.Th, and Tb.Sp in several areas of the condylar subchondral bone. Notably, BV/TV was significantly ($p < 0.01$) higher in the SHED-CM group ($0.42 \pm 0.05\%$) relative to the pre-treatment ($0.25 \pm 0.07\%$) and DMEM groups ($0.27 \pm 0.06\%$). The SHED-CM group also had a higher Tb.Th value ($0.16 \pm 0.08 \mu\text{m}$) compared to the pre-treatment ($0.09 \pm 0.02 \mu\text{m}$) and DMEM groups ($0.11 \pm 0.03 \mu\text{m}$), with a significant difference ($p < 0.05$) noted between the SHED-CM and DMEM groups. Concurrently, Tb.Sp was significantly ($p < 0.05$) smaller in the SHED-CM group ($0.21 \pm 0.11 \mu\text{m}$) relative to the pre-treatment ($0.39 \pm 0.25 \mu\text{m}$) and DMEM groups ($0.32 \pm 0.17 \mu\text{m}$) [Fig. 1 (F)].

SHED-CM suppressed masticatory muscle inflammation and pain and restored cellular alignment and matrix deposition of articular cartilage after TMJOA

Hematoxylin staining showed a massive infiltration of mononuclear immune cells into the damaged temporal muscle (TM) in the DMEM group, whereas the SHED-CM treated group exhibited markedly decreased infiltration. Of note, the inflammatory response in the synovial membrane (SM) in both the DMEM and SHED-CM groups was weak, suggesting the non-inflammatory nature of our mechanical stress-induced TMJOA model compared to the strong inflammatory nature of rheumatoid arthritis and synovitis [Fig. 2 (A)]. We further examined the effects of SHED-CM for TMJOA-induced mechanical hyper-nociception using the von Frey microfilament procedure. We found that SHED-CM treatment significantly suppressed TMJOA-induced hypersensitivity as indicated by reduced pain following SHED-CM treatment [Fig. 2 (B)].

Regarding the mandibular condyles, both pre-treatment and DMEM groups showed obvious OA-like lesions, such as a decrease in the condylar cartilage layer thickness and hyalinization of the cartilaginous matrix, and an increase in chondrocyte alignment irregularities. In contrast, the condylar cartilage of the SHED-CM group was similar to that of the sham control group, displaying obviously distinguished cell layers [Fig. 2 (C)]. Toluidine blue stained sections demonstrated that the proteoglycan positive area was significantly ($p < 0.01$) decreased in the pre-treatment and DMEM groups, accompanied with marked morphological changes. Meanwhile, condyles in the SHED-CM group were similar to those in the sham control [Fig. 2 (C) and (E)]. Modified Mankin morphological scores were significantly lower ($p < 0.01$) in the mandibular condylar cartilage samples from the SHED-CM group compared to those from the pre-treatment and DMEM groups [Fig. 2 (D)].

To evaluate the adverse side-effects of CM-treatment, we examined plasma CRP levels. We found that there were no significant differences between the CRP levels of the sham operated, pre-treatment, DMEM-treated, and SHED-CM-treated groups [Supplemental Table 1].

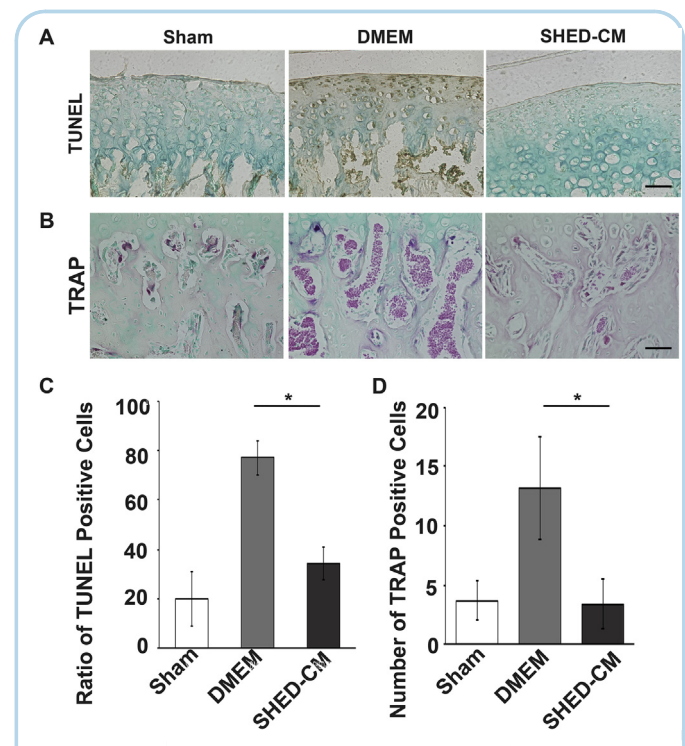


Fig. 3

SHED-CM suppresses chondrocyte apoptosis and osteoclast activity. Representative TMJ images of TUNEL-stained (A) and TRAP-stained (B) cells. Scale bar: 100 μm . Quantitative analysis of TUNEL positive (C) and TRAP positive cells (D). Data represent the mean \pm s.e.m. ($n = 5$). * $p < 0.05$.

SHED-CM suppressed osteoclastogenic activity in the subchondral bone layers of condyles

TRAP-positive osteoclasts were observed in the mineralized subchondral bone layers of mandibular condyles [Fig. 3 (B)]. The subchondral bone samples from the DMEM group (13.20 ± 4.36) exhibited significantly higher numbers of TRAP-positive cells ($p < 0.01$) relative to those from the SHED-CM (3.40 ± 2.06) and control groups (3.67 ± 1.70) [Fig. 3 (D)]. Taken together, this indicates that SHED-CM administration might downregulate osteoclastogenesis, leading to a decrease in bone resorption.

SHED-CM inhibited chondrocyte apoptosis in the subchondral bone of condyles

TUNEL assays were performed to determine whether apoptosis of abnormal chondrocytes was preferentially induced in degraded cartilage [Fig. 3 (A)]. An obvious increase in the number of TUNEL positive cells was observed in the DMEM group (76.97 ± 11.18 %) compared to the SHED-CM group (34.26 ± 6.97 %) [Fig. 3 (C)]. SHED-CM injection led to a decrease in TUNEL positive cells, thus providing a protective effect against cartilage degradation.

SHED-CM suppressed the expression of cartilage degradation-associated factors and promoted the proliferation of multipotent polymorphic cells

Immunohistological analysis showed that expression of the pro-inflammatory factor IL-1 β (95.56 ± 2.02 %) and cartilage matrix degradation factors MMP-13 (44.43 ± 7.90 %) and iNOS (48.8 ± 3.96 %) were elevated in the DMEM group when compared to the sham treated control (IL-1 β ; 79.96 ± 4.81 %, MMP-13; 26.69 ± 1.52 %, iNOS; 38.96 ± 1.63 %) [Fig. 4(A) and (B), (D), (E), (H), (I) and (N)]. The number of cells found positive for these factors increased in both multipotent polymorphic cells and the mature chondrocyte layer. In contrast, signal intensities of those exacerbating factors were reduced (IL-1 β ; 80.60 ± 4.95 %, MMP-13; 32.15 ± 5.78 %, iNOS; 38.72 ± 2.52 %) in the SHED-CM group [Fig. 4 (C), (F), (J) and (N)]. Furthermore, the majority of multipotent polymorphic cells were negative for these factors. Importantly, we found that PCNA-positive proliferating polymorphic cells were markedly increased in the SHED-CM treated group (sham group; 11.92 ± 3.40 %, DMEM group; 5.95 ± 2.70 %, SHED-CM group; 45.13 ± 4.56 %) [Fig. 4(K)–(N)]. These findings suggest that SHED-CM administration can protect against cartilage destruction and enhance cartilage formation in patients with TMJOA.

Secretome analysis of conditioned medium

Secretome analysis of SHED-CM resulted in the identification of 1,426 proteins. According to Gene Ontology cellular component classification, the number of cell surface, extracellular, or membrane proteins was 894. SHED-CM contained 51 of these proteins at levels at least 10 times greater than detected in Fibro-CM [Fig. 5 and Supplemental Fig. 2]. These molecules are known to be involved in the processes of anti-fibrosis, anti-apoptosis, anti-inflammation, proliferation, differentiation, and migration of chondrocytes.

Discussion

We previously reported on the therapeutic effects of systemically administrated SHED-CM against anti-collagen type II antibody-induced arthritis (CAIA)¹⁹. However, no study to date has examined the effect of SHED-CM administration against TMJOA. To the best of our knowledge, this is the first study reporting on the

promising potential of SHED-CM administration as an effective treatment of TMJOA. In this study, we used a mechanical-stress induced TMJOA model consisting of five consecutive days of TMJ damage followed by treatment with DMEM or CM for the next five days of TMJ damage. The initial TMJ damage induced pain and reduced condylar cartilage thickness and matrix deposition. Subsequent DMEM treatment worsened the pathophysiology of TMJOA. In contrast, SHED-CM treatment reduced pain and repaired osteoarthritic TMJ through the inhibition of the pro-inflammatory response, apoptosis, and matrix degradation while enhancing proliferation and matrix deposition of the cartilage layer. Our study revealed the remarkable articular cartilage regeneration activity of SHED-CM, which restored homeostasis in the mechanically destroyed TMJ.

Similar to previous studies, the TMJOA experimental model in the present study was established by applying mechanical stress to the mandibular condyle^{21,24–29}. This model was characterized by OA-like degenerated lesions, chondrocyte alignment irregularities in the condylar cartilage layers, subchondral bone loss, and marked depletion of proteoglycans. Furthermore, these results were consistent with results previously reported for early TMJOA generated by surgical manipulation of the joint^{30,31}, local application of chemicals^{32,33}, and genetic modification^{34,35}. Unlike rheumatoid arthritis and synovitis, TMJOA has a primarily non-inflammatory origin^{36,37}. The pathological process in TMJOA is characterized by deterioration and abrasion of the articular cartilage and local thickening and remodeling of the underlying bone³⁶. These changes are frequently accompanied by the superimposition of secondary inflammatory reactions. Surgical, genetic, or chemical methods cannot successfully mimic the real conditions encountered in patients with TMJOA, because of the high inflammatory arthritic conditions present in these induced animal models. Excessive mechanical stress is characterized as a key factor inducing mandibular condylar cartilage degradation in the TMJ. Therefore, our mechanical stress protocol of forced mouth opening is a useful tool for generating an experimental TMJOA model that can be used to evaluate the initiation and advancement of TMJOA.

Our data show that systemic intravenous administration of SHED-CM effectively repaired the lesions induced by TMJOA. Local injection allows for lower drug dosages and elicits fewer side effects, both systemic and local, when compared to conventional systemic intravenous injection. However, the needle pricks for local intra-articular injection can cause substantial tissue damages in TMJ. Our data show that the level of CRP in the SHED-CM treated group was similar to that of the sham-operated group, indicating there were little to no adverse side-effects after CM-treatment. Moreover, a small volume of systemic CM injection effectively restored injured TMJ. Taken together, systemic CM injection may avoid the iatrogenic disorders caused by needle pricks and provide considerable advantages in a clinical setting.

We characterized the soluble factors in SHED-CM by performing a LC-MS/MS analysis and found that SHED-CM contained 51 of the array proteins at levels more than 10-fold higher than those detected in Fibro-CM. A cluster analysis of these proteins identified 12 proteins known to provide beneficial effects in treating TMJOA and OA (Fig. 5). For instance, the identified insulin-like growth factor (IGF) and hepatocyte growth factor (HGF) are multifunctional proteins that protect cells from apoptosis and suppress inflammatory reactions. In cartilage repair, IGF promotes proliferation and maturation of chondrocytes, and the synthesis of their extracellular matrix. In bone remodeling, IGF enhances osteoblastogenesis, matrix deposition, and mineralization^{38,39}. Although the circulating half-life of the free form of IGF is reported to be around 10 min, IGF binding protein 5 (IGFBP-5) may form a complex with IGF in SHED-CM and extend its half-life⁴⁰. HGF enhances cellular motility,

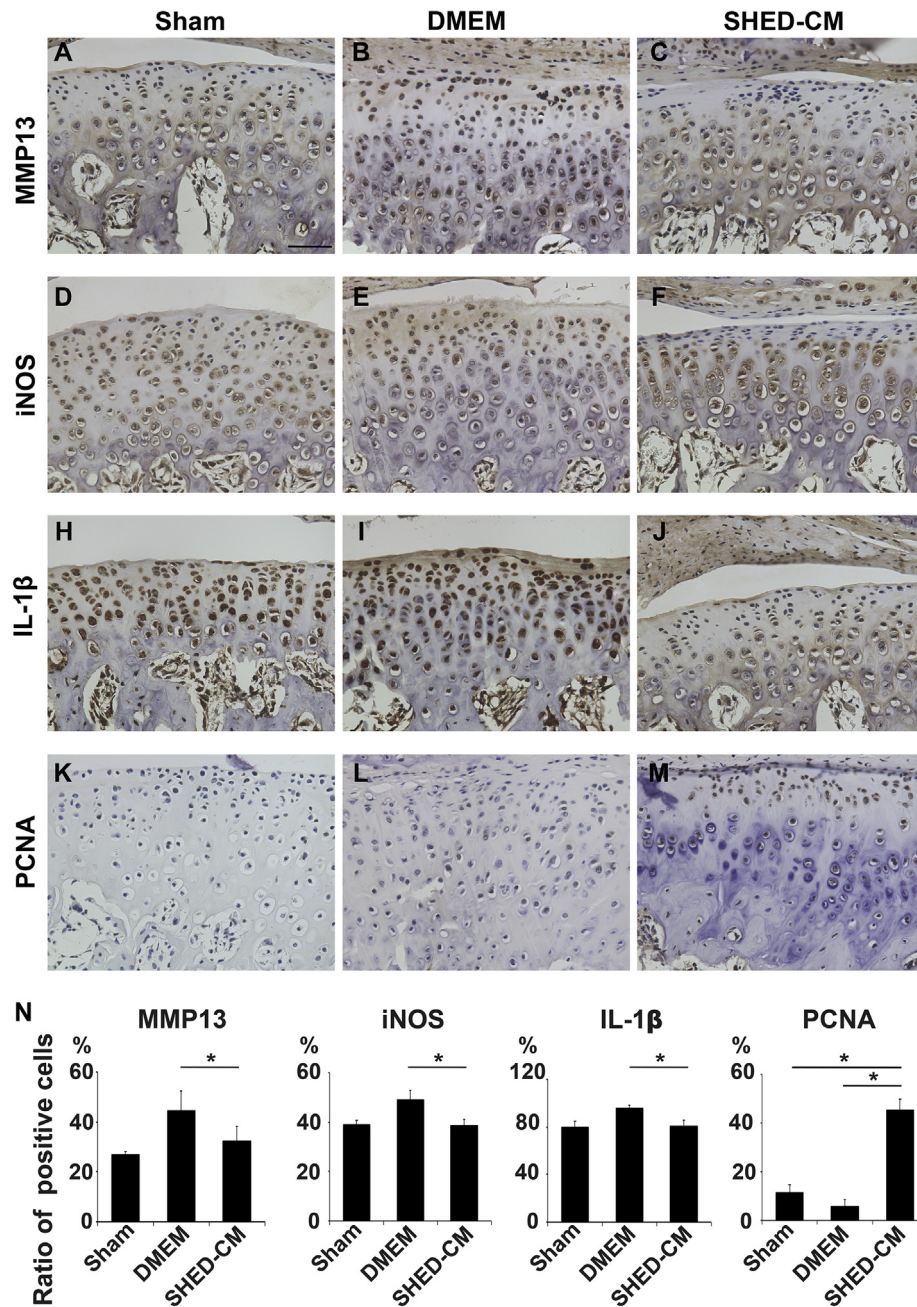


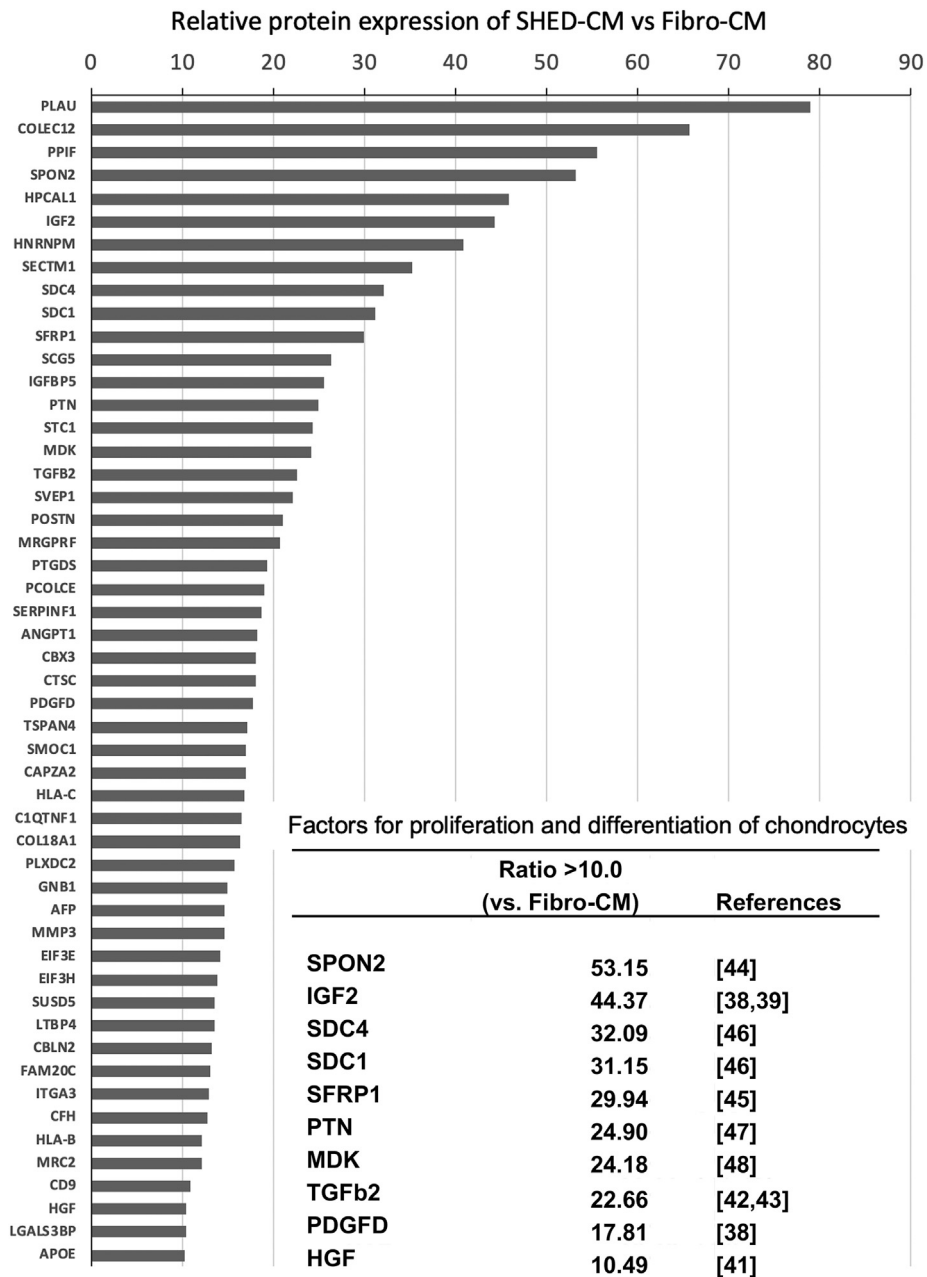
Fig. 4

SHED-CM suppresses inflammation and promotes cellular proliferation during TMJ repair. Representative images for quantitative analysis of cells stained for (A) MMP13 (B) iNOS (C) IL-1β at 3 days and (D) PCNA at 7 days in TMJ condylar cartilage. Scale bar: 100 μm. The number of cells stained positive for MMP13, iNOS, IL-1β and PCNA were counted at 200× magnification and expressed as percentages of positively stained cells. Data represent mean ± s.e.m. (n = 5/group). *p < 0.05.

Osteoarthritis and Cartilage

proliferation, and proteoglycan synthesis of chondrocytes and activates osteoblast for bone regeneration⁴¹. Transforming growth factor β (TGF-β) promotes the differentiation of chondrocytes and the synthesis of collagen and proteoglycans, thereby maintaining cartilage homeostasis^{42,43}. R-Spondin 2 (SPON2), an activator of Wnt/β-catenin signaling, promotes endochondral ossification through induction of chondrogenic differentiation⁴⁴. Secreted frizzled related protein 1 (SFRP1), a Wnt signaling antagonist, is

required for the maintenance of immature proliferating chondrocyte precursors⁴⁵. Syndecan (SDC), a cell surface heparan sulphate proteoglycan, promotes chondrocyte proliferation and maintains cartilage matrix homeostasis⁴⁶. Platelet derived growth factor (PDGF), is a potent mitogenic and chemotactic factor for all mesenchymal originating cells, including chondrocytes and MSCs³⁸, while pleiotrophin (PTN) and midkine (MDK) are involved in the mitotic activation of chondrocytes^{47,48}. It has been reported

**Fig. 5**

LC-MS/MS analysis of SHED-CM and Fibro-CM. In SHED-CM, a total of 1,426 proteins were identified. From these, 51 proteins were more than 10 times higher in SHED-CM compared to the Fibro-CM.

Osteoarthritis
and Cartilage

that MDK, a heparin-binding growth factor, promotes the proliferation of articular chondrocytes *in vivo* when administrated subcutaneously in normal mice⁴⁸, suggesting that systemically administrated MDK may reach the joint. Despite the relatively low concentrations of chondrogenic factors (1–10 ng/ml) measured in SHED-CM, the combinatorial effects of these multiple factors may provide prominent therapeutic benefits in treating TMJOA. To clarify the detail mechanisms of SHED-CM-mediated articular cartilage regeneration, in future it is necessary to examine the accessibility of therapeutic factor in SHED-CM toward injured TMJ.

Recent reports have revealed that MSCs-derived extracellular vesicles (EVs) play important roles in the trophic effects exhibited in MSCs-transplantation therapy. Importantly, several studies have demonstrated a cartilage regenerating activity of MSCs-derived exosomes, a type of EVs released from cells through fusion of endosomal multivesicular bodies with the plasma membrane⁴⁹. Exosomes carry multiple heterogeneous proteins, micro-RNAs and lipids, which are involved in many diverse biochemical and cellular processes, such as communication, structure and mechanics, inflammation, exosome biogenesis, tissue repair and regeneration,

and metabolism. Exosomes express endosome-related proteins, such as Alix, tumor susceptibility 101 (TSG101), integrin α chains, and tetraspanins (TSPANs, CD9, CD63, CD81), which are members of a protein superfamily characterized by the presence of four transmembrane and two extracellular domains⁵⁰. In the list obtained from our SHED-CM proteome analysis, we identified many exosome markers, such as TSPAN 4, CD9, and Integrin α 3 (ITGA3), suggesting that SHED cells may produce a larger number of exosomes than previously thought. In the future, it would be necessary to clarify the roles of exosomes and trophic factors in SHED-CM-mediated cartilage and bone regeneration of the mandibular condylar.

As previously described, TMJOA is characterized by mandibular condylar cartilage degradation due to mechanical stress². Mechanical stress of the mandibular condylar cartilage induces the expression of IL-1 β , an inflammatory cytokine closely related to the progression of TMJOA³. Since the fibrocartilage covering both the mandibular condyle and articular eminence is avascular, these fibrocartilage cells have limited ability for self-repair, similar to the hyaline cartilage in other synovial joints⁵¹. Therefore, once the breakdown in the joint starts, TMJOA can be crippling, leading to a variety of morphological and functional deformities. This highlights the importance of suppressing cartilage degradation during the early stages of TMJOA. However, so far no treatment remedy has been developed for the management of severe TMJOA. Furthermore, despite the fact that many studies have demonstrated the potential of using embryonic stem (ES) cells for cartilage regeneration, many concerns raised by the use of ES cells, such as possible tumorigenesis, ethical issues regarding the use of embryos and potential allogeneic immune rejection, make this approach problematic. The use of induced pluripotent stem (iPS) cells may overcome most of these issues. However, this technology is still in its infancy and includes many unknown parameters. In the present study, we used SHED-CM for the treatment of TMJOA through cartilage regeneration and our results suggested that SHED-CM administration can attenuate cartilage degeneration, promote cartilage regeneration, and protect against the progression of TMJOA induced by mechanical stress. Therefore, SHED-CM administration may represent an effective treatment strategy for patients with mechanical stress-induced TMJOA.

In conclusion, we showed that SHED-CM contained multiple therapeutic factors with the potential for treating TMJOA. Importantly, we did not observe any adverse side-effects during the experimental treatment period. Our findings suggest that SHED-CM not only inhibited the articular degradation cascade but also regenerated the injured articular by promoting proliferation of the multipotent polymorphic cell layer and production of cartilage matrix in mice with TMJOA. Thus, SHED-CM may provide a novel articular regenerative therapy for patients with severe TMJOA.

Studies involving humans or animals

This study was approved by the Institutional Ethical Committee of Nagoya University and Tokushima University Hospital and performed according to the principles of Helsinki Declaration (Permit No H-73 and No: 3,268 for Nagoya and Tokushima University, respectively). All procedures performed in this study involving animals were approved by the Tokushima University Animal Care and Use Committee (Permit No: T30-95).

Contributions

Study conception and design: NO, ET, AY. Acquisition of data: NO, FK, NH, HM, YL, LX, TS. Provision of study materials or patients: HH, TI. Analysis & interpretation of data: All authors. Writing of first

manuscript draft: NO, ET, AY. Critical manuscript revision and approval of final manuscript: All authors. AY had full access to all of the data in the study and takes responsibility for the integrity of the data and the accuracy of the data analysis.

Conflict of Interest

The authors declare that there is no conflict of interest.

Funding sources

This work was supported by Grants-in-Aid for Scientific Research on Priority Areas from the Ministry of Education, Culture, Sports, Science and Technology of Japan (22390372).

Acknowledgments

We are grateful to N. Ishimaru and H. Kosako for instructive pathological comments and LC-MS/MS analysis, respectively. We thank the Division of Experimental Animals and Medical Research Engineering, Tokushima University Graduate School, for housing the animals and for providing microscope maintenance. We thank to the support center for advanced medical sciences, Tokushima University Graduate School of biomedical Sciences for CT analysis.

Supplementary data

Supplementary data to this article can be found online at <https://doi.org/10.1016/j.joca.2020.03.010>.

References

- Mizoguchi I, Toriya N, Nakao Y. Growth of the mandible and biological characteristics of the mandibular condylar cartilage. *Jpn Dent Sci Rev* 2013;49:139–50.
- Tanaka E, Detamore MS, Mercuri LG. Degenerative disorders of the temporomandibular joint: etiology, diagnosis, and treatment. *J Dent Res* 2008;87:296–307.
- Kuroda S, Tanimoto K, Izawa T, Fujihara S, Koolstra JH, Tanaka E. Biomechanical and biochemical characteristics of the mandibular condylar cartilage. *Osteoarthritis Cartilage* 2009;17:1408–15.
- Wang XD, Zhang JN, Gan YH, Zhou YH. Current understanding of pathogenesis and treatment of TMJ osteoarthritis. *J Dent Res* 2015;94:666–73.
- Cui D, Li H, Xu X, Ye L, Zhou X, Zheng L, et al. Mesenchymal stem cells for cartilage regeneration of TMJ osteoarthritis. *Stem Cell Int* 2017;2017:5979741.
- De Bari C, Roelofs AJ. Stem cell-based therapeutic strategies for cartilage defects and osteoarthritis. *Curr Opin Pharmacol* 2018;40:74–80.
- Konala VB, Mamidi MK, Bhonde R, Das AK, Pochampally R, Pal R. The current landscape of the mesenchymal stromal cell secretome: a new paradigm for cell-free regeneration. *Cytotherapy* 2016;18:13–24.
- Sakai K, Yamamoto A, Matsubara K, Nakamura S, Naruse M, Yamagata M, et al. Human dental pulp-derived stem cells promote locomotor recovery after complete transection of the rat spinal cord by multiple neuro-regenerative mechanisms. *J Clin Invest* 2012;122:80–90.
- Mata M, Milian L, Oliver M, Zurriaga J, Sancho-Tello M, de Llano JJM, et al. In vivo articular cartilage regeneration using human dental pulp stem cells cultured in an alginate scaffold: a preliminary study. *Stem Cell Int* 2017;2017:1–9.
- Yamamoto A, Sakai K, Matsubara K, Kano F, Ueda M. Multi-faceted neuro-regenerative activities of human dental pulp

- stem cells for functional recovery after spinal cord injury. *Neurosci Res* 2014;78:16–20.
11. Yamagata M, Yamamoto A, Kako E, Kaneko N, Matsubara K, Sakai K, et al. Human dental pulp-derived stem cells protect against hypoxic-ischemic brain injury in neonatal mice. *Stroke* 2013;44:551–4.
 12. Mita T, Furukawa-Hibi Y, Takeuchi H, Hattori H, Yamada K, Hibi H, et al. Conditioned medium from the stem cells of human dental pulp improves cognitive function in a mouse model of Alzheimer's disease. *Behav Brain Res* 2015;293:189–97.
 13. Matsubara K, Matsushita Y, Sakai K, Kano F, Kondo M, Noda M, et al. Secreted ectodomain of sialic acid-binding Ig-like lectin-9 and monocyte chemoattractant protein-1 promote recovery after rat spinal cord injury by altering macrophage polarity. *J Neurosci* 2015;35:2452–64.
 14. Matsushita Y, Ishigami M, Matsubara K, Kondo M, Wakayama H, Goto H, et al. Multifaceted therapeutic benefits of factors derived from stem cells from human exfoliated deciduous teeth for acute liver failure in rats. *J Tissue Eng Regen Med* 2017;11:1888–96.
 15. Hirata M, Ishigami M, Matsushita Y, Ito T, Hattori H, Hibi H, et al. Multifaceted therapeutic benefits of factors derived from dental pulp stem cells for mouse liver fibrosis. *Stem Cells Translational Medicine* 2016;5:1416–24.
 16. Wakayama H, Hashimoto N, Matsushita Y, Matsubara K, Yamamoto N, Hasegawa Y, et al. Factors secreted from dental pulp stem cells show multifaceted benefits for treating acute lung injury in mice. *Cytotherapy* 2015;17:1119–29.
 17. Shimojima C, Takeuchi H, Jin S, Parajuli B, Hattori H, Suzumura A, et al. Conditioned medium from the stem cells of human exfoliated deciduous teeth ameliorates experimental autoimmune encephalomyelitis. *J Immunol* 2016;196:4164–71.
 18. Izumoto-Akita T, Tsunekawa S, Yamamoto A, Uenishi E, Ishikawa K, Ogata H, et al. Secreted factors from dental pulp stem cells improve glucose intolerance in streptozotocin-induced diabetic mice by increasing pancreatic beta-cell function. *BMJ Open Diabetes Res Care* 2015;3. e000128.
 19. Ishikawa J, Takahashi N, Matsumoto T, Yoshioka Y, Yamamoto N, Nishikawa M, et al. Factors secreted from dental pulp stem cells show multifaceted benefits for treating experimental rheumatoid arthritis. *Bone* 2016;83:210–9.
 20. Yamaguchi S, Shibata R, Yamamoto N, Nishikawa M, Hibi H, Tanigawa T, et al. Dental pulp-derived stem cell conditioned medium reduces cardiac injury following ischemia-reperfusion. *Sci Rep* 2015;5:16295.
 21. Izawa T, Mori H, Shinohara T, Mino-Oka A, Hutami IR, Iwasa A, et al. Rebamipide attenuates mandibular condylar degeneration in a murine model of TMJ-OA by mediating a chondroprotective effect and by downregulating RANKL-mediated osteoclastogenesis. *PloS One* 2016;11:e0154107–18.
 22. Ren K. An improved method for assessing mechanical allodynia in the rat. *Physiol Behav* 1999;67:711–6.
 23. Motani K, Kosako H. Activation of stimulator of interferon genes (STING) induces ADAM17-mediated shedding of the immune semaphorin SEMA4D. *J Biol Chem* 2018;293:7717–26.
 24. Fujisawa T, Kuboki T, Kasai T, Sonoyama W, Kojima S, Uehara J, et al. A repetitive, steady mouth opening induced an osteoarthritis-like lesion in the rabbit temporomandibular joint. *J Dent Res* 2003;82:731–5.
 25. Tanaka E, Aoyama J, Miyauchi M, Takata T, Hanaoka K, Iwabe T, et al. Vascular endothelial growth factor plays an important autocrine/paracrine role in the progression of osteoarthritis. *Histochem Cell Biol* 2005;123:275–81.
 26. Shirakura M, Tanimoto K, Eguchi H, Miyauchi M, Nakamura H, Hiyama K, et al. Activation of the hypoxia-inducible factor-1 in overloaded temporomandibular joint, and induction of osteoclastogenesis. *Biochem Biophys Res Commun* 2010;393:800–5.
 27. Jiao K, Wang MQ, Niu LN, Dai J, Yu SB, Liu XD, et al. Death and proliferation of chondrocytes in the degraded mandibular condylar cartilage of rats induced by experimentally created disordered occlusion. *Apoptosis* 2009;14:22–30.
 28. Sobue T, Yeh WC, Chhibber A, Utreja A, Diaz-Doran V, Adams D, et al. Murine TMJ loading causes increased proliferation and chondrocyte maturation. *J Dent Res* 2011;90:512–6.
 29. Zhang J, Jiao K, Zhang M, Zhou T, Liu XD, Yu SB, et al. Occlusal effects on longitudinal bone alterations of the temporomandibular joint. *J Dent Res* 2013;92:253–9.
 30. Xu L, Polur I, Lim C, Servais JM, Dobeck J, Li Y, et al. Early-onset osteoarthritis of mouse temporomandibular joint induced by partial disectomy. *Osteoarthritis Cartilage* 2009;17:917–22.
 31. Liu XW, Hu J, Man C, Zhang B, Ma YQ, Zhu SS. Insulin-like growth factor-1 suspended in hyaluronan improves cartilage and subchondral cancellous bone repair in osteoarthritis of temporomandibular joint. *Int J Oral Maxillofac Surg* 2011;40:184–90.
 32. Wang XD, Kou XX, He DQ, Zeng MM, Meng Z, Bi RY, et al. Progression of cartilage degradation, bone resorption and pain in rat temporomandibular joint osteoarthritis induced by injection of iodoacetate. *PloS One* 2012;7. e45036.
 33. Liu YD, Liao LF, Zhang HY, Lu L, Jiao K, Zhang M, et al. Reducing dietary loading decreases mouse temporomandibular joint degradation induced by anterior crossbite prosthesis. *Osteoarthritis Cartilage* 2014;22:302–12.
 34. Wadhwa S, Embree MC, Kilts T, Young MF, Ameye LG. Accelerated osteoarthritis in the temporomandibular joint of biglycan/fibromodulin double-deficient mice. *Osteoarthritis Cartilage* 2005;13:817–27.
 35. Embree M, Ono M, Kilts T, Walker D, Langguth J, Mao J, et al. Role of subchondral bone during early-stage experimental TMJ osteoarthritis. *J Dent Res* 2011;90:1331–8.
 36. Zarb GA, Carlsson GE. Temporomandibular disorders: osteoarthritis. *J Orofac Pain* 1999;13:295–306.
 37. de Souza Tesch R, Takamori ER, Menezes K, Carias RBV, Dutra CLM, de Freitas Aguiar M, et al. Temporomandibular joint regeneration: proposal of a novel treatment for condylar resorption after orthognathic surgery using transplantation of autologous nasal septum chondrocytes, and the first human case report. *Stem Cell Res Ther* 2018;9:1–12.
 38. Schmidt MB, Chen EH, Lynch SE. A review of the effects of insulin-like growth factor and platelet derived growth factor on in vivo cartilage healing and repair. *Osteoarthritis Cartilage* 2006;14:403–12.
 39. Yakar S, Werner H, Rosen CJ. Insulin-like growth factors: actions on the skeleton. *J Mol Endocrinol* 2018;61:T115–37.
 40. Twigg SM, Baxter RC. Insulin-like growth factor (IGF)-binding protein 5 forms an alternative ternary complex with IGFs and the acid-labile subunit. *J Biol Chem* 1998;273:6074–9.
 41. Yuan XL, Meng HY, Wang YC, Peng J, Guo QY, Wang AY, et al. Bone-cartilage interface crosstalk in osteoarthritis: potential pathways and future therapeutic strategies. *Osteoarthritis Cartilage* 2014;22:1077–89.
 42. Xu X, Zheng L, Yuan Q, Zhen G, Crane JL, Zhou X, et al. Transforming growth factor-beta in stem cells and tissue homeostasis. *Bone Res* 2018;6:2.

43. Patil AS, Sable RB, Kothari RM. An update on transforming growth factor- β (TGF- β): sources, types, functions and clinical applicability for cartilage/bone healing. *J Cell Physiol* 2011;226:3094–103.
44. Takegami Y, Ohkawara B, Ito M, Masuda A, Nakashima H, Ishiguro N, et al. R-spondin 2 facilitates differentiation of proliferating chondrocytes into hypertrophic chondrocytes by enhancing Wnt/beta-catenin signaling in endochondral ossification. *Biochem Biophys Res Commun* 2016;473:255–64.
45. Gaur T, Rich L, Lengner CJ, Hussain S, Trevant B, Ayers D, et al. Secreted frizzled related protein 1 regulates Wnt signaling for BMP2 induced chondrocyte differentiation. *J Cell Physiol* 2006;208:87–96.
46. Bertrand J, Stange R, Hidding H, Echtermeyer F, Nalesso G, Godmann L, et al. Syndecan 4 supports bone fracture repair, but not fetal skeletal development, in mice. *Arthritis Rheum* 2013;65:743–52.
47. Pufe T, Groth G, Goldring MB, Tillmann B, Mentlein R. Effects of pleiotrophin, a heparin-binding growth factor, on human primary and immortalized chondrocytes. *Osteoarthritis Cartilage* 2007;15:155–62.
48. Zhang ZH, Li HX, Qi YP, Du LJ, Zhu SY, Wu MY, et al. Recombinant human midkine stimulates proliferation of articular chondrocytes. *Cell Prolif* 2010;43:184–94.
49. Toh WS, Lai RC, Hui JHP, Lim SK. MSC exosome as a cell-free MSC therapy for cartilage regeneration: implications for osteoarthritis treatment. *Semin Cell Dev Biol* 2017;67:56–64.
50. Denzer K, Kleijmeer MJ, Heijnen HF, Stoorvogel W, Geuze HJ. Exosome: from internal vesicle of the multivesicular body to intercellular signaling device. *J Cell Sci* 2000;113(19):3365–74.
51. Iwamoto M, Ohta Y, Larmour C, Enomoto-Iwamoto M. Toward regeneration of articular cartilage. *Birth Defects Res C Embryo Today* 2013;99:192–202.